Numerical Wideband Anthropomorphic Phantom for Biomedical Microwave Imaging

N. Joachimowicz, Soroush Abedi, Hélène Roussel

Numerical Wideband Anthropomorphic Phantom for Biomedical Microwave Imaging

Joachimowicz Nadine
Laboratoire de Génie Electrique et Electronique de Paris (GeePs)
Sorbonne Université, CNRS
Paris, France
nadine.joachimowicz@paris7.jussieu.fr

Abedi Soroush
Laboratoire de Génie Electrique et Electronique de Paris (GeePs)
Sorbonne Université, CNRS
Paris, France
abedi.soroush@gmail.com

Roussel Hélène
Laboratoire de Génie Electrique et Electronique de Paris (GeePs)
Sorbonne Université, CNRS
Paris, France
helene.roussel@sorbonne-universite.fr

***Abstract*—In this work, the advantages of 3D printed anthropomorphic phantoms applied to the assessment of microwave imaging devices and the potential contribution of their numerical version for microwave imaging are examined. Three phantoms that represent main body areas are used for illustration: head, breast and thorax. The context of the analysis deals with dynamic imaging where several data sets are taken from a body at different moments and the image is reconstructed from the difference in the scattered field recorded. The work is focused on the effect of a local change of the dielectric properties on the differential field distribution and constitutes an example of what can be done with the numerical version of the 3D printed anthropomorphic phantoms.**

Keywords—wideband anthropomorphic phantoms, qualitative microwave imaging, tumors, strokes monitoring

I. INTRODUCTION

In microwave imaging, the quantity reconstructed is the dielectric contrast of the object or the induced currents created in it, for quantitative and qualitative imaging respectively. Monitoring, control during hyperthermia treatments mean that interests are focused on a local change of dielectric properties distribution and qualitative imaging can be attractive to overcome the no linearity of the inverse scattering problem that has to be solved. However, one of the drawbacks of qualitative microwave imaging is that the induced currents, referred to as J, depend both on the dielectric properties and the total field inside the object. Indeed, at the first order, we can consider that, $\Delta J = E\,\Delta c + c\,\Delta E$ (1), if c and Δc denote the dielectric contrast and its variation respectively. This equation shows that the local change of the complex permittivity results in two terms. The first one is directly proportional to the change of the dielectric contrast and, hence is expected to provide some modification on the image exactly where the local permittivity change is. The second term is dependent on ΔE, and then is not necessarily located in the region where the dielectric properties change is and some artifacts may result. This raises the question of the relevance of qualitative differential imaging for monitoring and hyperthermia applications. In this work, the distribution of the differential field ΔE is investigated with the numerical version of anthropomorphic phantoms to address this question in realistic situations. The flowchart of the benchmark phantoms develop by our group is first introduced in section 2. Next, a new 3D printed axillary phantom is described in section 3. Section 4 is devoted to the numerical simulations through some examples of the differential field distribution in the anthropomorphic phantoms that represent the thorax the head, and the breast. Section 5 gives the image of the GeePS-L2S breast phantom [1] produced in real-time by the microwave camera [2].

II. A SIMULATION BASED METHODOLOGY

The process of developing 3D printed phantoms is based on a simulation methodology [3]. As an example, Figure 1 represents the flowchart of the process for an anthropomorphic head phantom. Steps (I), (II) and (III) provide a numerical file of the phantom composed of anthropomorphic cavities, thanks to the primary IRM scan. The cavities are designed using CAD software in order to match the microwave imaging device and to be fillable with TMMs (Step IV), whose recipes are given numerically by an optimization process [1, 3]. A website providing the recipe to mimick a given biological tissue in the microwave frequency range is under development.

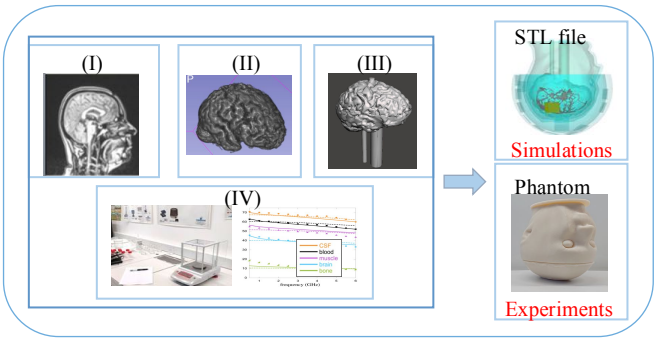

Fig 1. 3D printed head phantom flowchart

The 3D printed phantom filled with TMM can be used for experiments as it has been done in [4]; its numerical version can be up-load into a forward solver to simulate data of the microwave imaging problem, for the investigation of the device (source, frequency, coupling medium...) and the phantom itself (design, cavities material…) [3], as well as into several inverse solvers to compare their efficiency for example. This constitutes the main advantage of this type of phantom: the ability to perform experimental validations on anthropomorphic objects associated with numerical simulations. This work is focused on the effect of a numerical local change of the dielectric properties, on the differential field distribution for three anthropomorphic printed phantoms. The first considered is the thorax phantom.

III. A 3D PRINTED THORAX PHANTOM

This section gives the description of the new 3D printed phantom "SIMONE". The cavities (Figure 2) are designed from a Plasticboy Anatomy Model [5] and modified by CAD software in order to be printable, liquid-fillable and cleanable. The lung cavity fixed inside the muscle cavity is filled through two cylinders attached to it. The bone part that represents the scapula and humerus (upper arm) is made of printable material. Elliptical cavities of different sizes have been added to represent the lymph nodes. The elliptical cavities are connected by a plastic pipe, so they can be filled from outside to simulate a change in dielectric properties over time. The tub is fixed to the skin cavity with clips, one of which is visible in figure 2. Note that, the thorax phantom is herein designed for the detection of axillary nodes but the phantom can be used for lung tumor detection as well for example, if tumor cavities are placed in the pipes connected to the lung. This is another advantage of phantom with 3D printed cavities.

Fig 2. The axillary region phantoms including cavities designed from plasticboy anatomy models [5].

IV. NUMERICAL SIMULATIONS WITH A PLANE WAVE ILLUMINATION

The computation of the electromagnetic field (EM) distribution is done using the commercial software CST Microwave-Studio. The differential field distribution is obtained by substracting the field obtained in the presence of the anomaly from that obtained in its absence and is given in V/m in the figures. The values of the dielectric properties for muscle, lung, lymph, CSF, bone, and blood tissues are published in [6].

The chest phantom consists of an outer shell of muscle containing the lung and lymph nodes and a piece of bone. The bone tissue is made of 3D printed material (ABS). The phantom is illuminated by an incident plane wave on the front of the thorax at 1 GHz, in free space.

As it is shown in Fig. 3a and Fig.3b, a difference of size instead of dielectric properties between malignant and healthy nodes is considered, since a lymph node that grows in size is pathological.

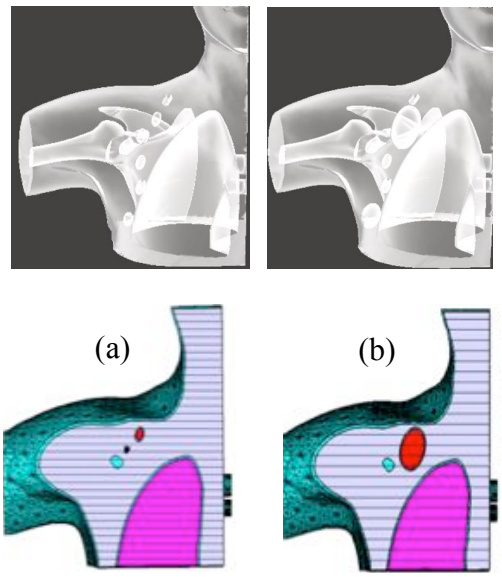

Fig 3. Thorax phantom and the cross section including (a) healthy and (b) pathologic lymph nodes

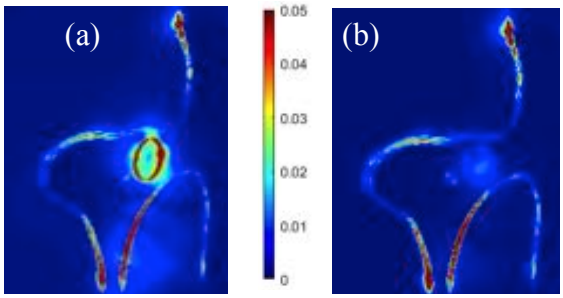

Fig 4. Magnitude of the differential field distribution inside the thorax phantom including nodes cavity (a) in ABS, (b) muscle tissue.

Figure 4 shows the magnitude of the differential field distribution between pathological (3b) and non-pathological (3a) thorax phantom when the nodes cavity are made (a) in ABS and (b) in a printed material whose dielectric properties are similar to the muscle tissue. It appears that the lymph nodes are visible from the local variation of the E-field distribution in both cases (Figure 4 (a,b)) despite the low dielectric contrast of approximatively 10% between the muscle and the lymph node. This result will be confirmed for higher dielectric contrast with the 2 following anthropomorphic phantoms developed in our previous works [1]. The GeePs head phantom developed in the frame of the POLITO device [4] is herein illuminated in free space by a plane wave at 1 GHz. It contains three cavities whose dielectric properties are CSF (brown), brain (blue) and blood for the stroke (red) according to Figure 5a. The GeePs-L2S breast phantom [1] is herein studied in the configuration of the planar camera [2] that operates at 2.45 GHz, in water at 37°C. The phantom is composed of fatty (blue), glandular (violet) and tumor (green) parts (Figure 5b).

The magnitude of the differential field distributions inside the head phantom with a spherical stroke and the breast phantom with a cylindrical tumor are represented in figure 5c and 5d respectively. As previously observed, the magnitude of the differential field is maximum at the location of anomalies, making them visible.

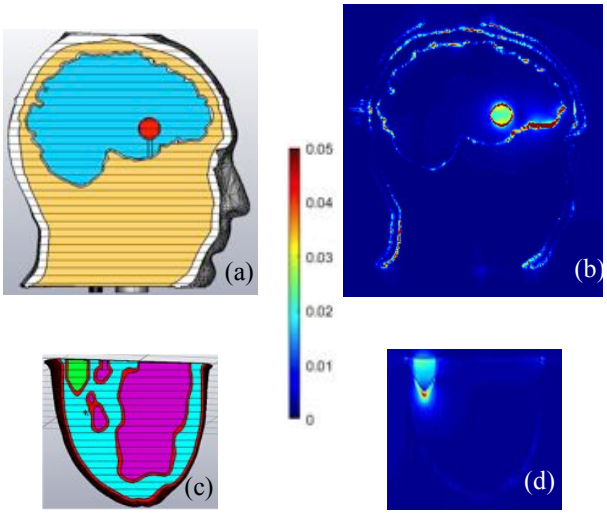

Fig 5. (a) the GeePs head phantom including a spherical stroke cavity, (b) the GeePs-L2S breast phantom including a cylindrical tumor cavity [1], and (c), (d) the corresponding magnitude of the differential field distribution.

V. Experiments with the Microwave Camera

The GeePs-L2S breast phantom was introduced in the planar camera developed by our group a few decades ago [7,8]. The camera is coupled to a diffraction tomography algorithm that provides real-time images representing the distribution of induced currents J in different planes of the object [9]. Figure 6(a) shows a plane through the tumor and 6(b) the corresponding differential image. In figure 6(b), the hot spot which could be associated to the tumor, is outside the breast, but the inhomogeneity of the phantom and the complex shape of the glandular part are rather well reproduced in Figure 6 (a). The use of a spectral extrapolation algorithm such as Gerchberg Papoulis [10] based on the introduction of the breast contour as a priori information [11] or a multi-incidence configuration [12], are some examples of avenues to be explored to improve the spatial resolution of the microwave camera images and the quality of the differential image.

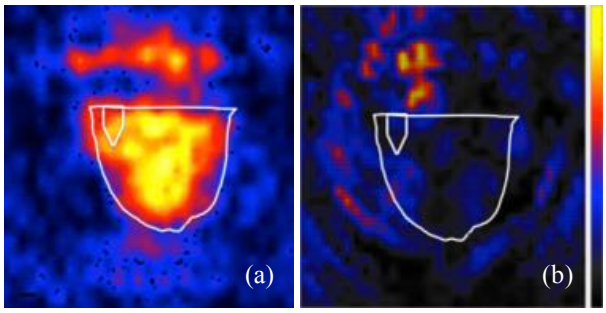

Fig 6. The images provide by the camera : (a) the induced current distribution, (b) the differential image, in a cross section of the tumor.

VI. Conclusion

In this study, the effect of a local change in the complex permittivity of anthropomorphic phantoms was investigated in order to validate in realistic situations the use of differential qualitative imaging for monitoring and hyperthermia applications. For the three cases considered, it appeared that in theory, this change locally induced effectively a modification in the distribution of the electric field at the same location. This work was placed in a plane wave configuration, but some other simulations carried out within the framework of the imaging system developed in [4] led to the same result [3]. The quantity ΔJ as well as ΔE, seems to be proper quantities to track the status of the anomaly over time in those examples. However, experiments with the microwave camera failed for the breast phantom. One reason for this could be the limited spatial resolution of the images at lambda/2 in

diffraction tomography. Future works will focus on the reduction of the high-computational cost of the microwave imaging algorithms, in order to introduce such anthropomorphic models in inverse scattering solvers such as that developed in [13]. Work on the optimal mesh and simplified phantom design will be preliminary [14]. The use of the multi-incidence and/or multi-view measurements as well as the introduction of contours as a priori information in the scattering solver in order to improve the resolution of the microwave images will also be investigated.

ACKNOWLEDGMENT

This work was funded by the EMERALD project funded from the European Union's Horizon 2020 research and innovation program under the Marie Skłodowska-Curie grant agreement No. 764479.

REFERENCES

[1] N. Joachimowicz, B. Duchêne, C. Conessa, and O. Meyer, 2018. "Anthropomorphic breast and head phantoms for microwave imaging". Diagnostics, 8 (4) : 85, 2018

[2] T. Henriksson, N. Joachimowicz, C. Conessa, J.Ch. Bolomey, "Quantitative Microwave Imaging for Breast Cancer Detection Using a Planar 2.45 GHz System," IEEE Trans. Instrum. Meas., 59, pp. 2691-2699, 2010

[3] S. Abedi, N. Joachimowicz, N. Philips and H. Roussel, "A Simulation-based methodology of developing 3D printed anthropomorphic phantoms for microwave imaging systems," Diagnostics, 11(2) : 376, 2021

[4] A. Tobon Vasquez, R. Scapaticci, G.Turvani, G., Bellizzi, D. O. Rodriguez-Duarte, N. Joachimowicz, B. Duchêne, E. Tedeschi, M.R.Casu, L. Crocco, and F. Vipiana,, "A Prototype Microwave System for 3D Brain Stroke Imaging". Sensors, 20, 9, pp. 2607, 2020

[5] Plasticboy. Available online: (accessed on 5.7.2021): https://www.plasticboy.co.uk/store/index.html.

[6] IFAC. Available on line (accessed on 28.5.2020): http://niremf.ifac.cnr.it/tissprop/htmlclie/htmlclie.php

[7] J.Ch. Bolomey, L. Jofre and G. Peronnet "On the Possible Use of Microwave-Active Imaging for Remote Thermal Sensing," IEEE Trans. Microw. Theory Techn., Vol-31, No. 9, pp. 777-781, September 1983

[8] C. Pichot, L. Jofre, G. Peronnet, J.C. Bolomey, "Active microwave imaging of inhomogeneous bodies". IEEE Trans. Antennas Propag. **33**, 416–425, 1985

[9] A. Joisel, J. C. Bolomey, "Rapid microwave imaging of living tissues". Proc. SPIE **3977**, 320– 330, 2000

[10] A. Papoulis, "A new algorithm in spectral analysis and bandlimited extrapolation", IEEE Trans. Circ. Sys., **9**, 734–741, 1975

[11] W. Tabbara, B. Duchêne, Ch Pichot, D. Lesselier, L. Chommeloux, N. Joachimowicz, "Diffraction Tomography : Contribution to the analysis of some applications in microwaves and ultrasonics, Invesre Problem", 4(2) :305, 1999

[12] A. Diaz-Bolado, T. Henriksson, P.A. Barriere, H. Memarzadey-Tehran, N. Joachimowicz, C. Conessa, A. Joisel, J.Ch. Bolomey, "Towards a planar microwave tomography system for early stage breast cancer detection", URSIGASS 2011, DOI:10.1109/URSIGASS.2011.6051368

[13] R. Scapaticci, O. M. Bucci, I. Catapano, and L. Crocco, "Differential Microwave Imaging for Brain Stroke Followup," *International Journal of Antennas and Propagation*, vol. 2014, Article ID 312528, 11 pages, 2014

[14] T. Singh, S. Abedi, S., B. Nikovic., M. Stevanovic, N. Joachimowicz, H. Roussel, B. Kolundzjja, "Smart simplification of Anthropomorphic Head Phantom Aimed for Microwave imaging." 15th European Conference on Antenna and Propagation (EuCAP), 2021